MIMO conditional integrator control for a class of nonlinear systems

Gilney Damm, van Cuong Nguyen

MIMO Conditional Integrator Control for a Class of Nonlinear Systems

Gilney Damm and Van Cuong Nguyen

Abstract— **This work develops a Multi-Input Multi-Output (MIMO) Conditional Integrator (CI) controller to a class of MIMO nonlinear systems, in the case of asymptotically constant references, motivated by airspace applications. These results are then applied to an aircraft control case and are compared by computer simulations with previous results from the literature that represent the starting point of the current paper.**

The obtained controller allows in a first step finite time semiglobal stability to a residual region, followed by exponential stability since entering this region.

I. Introduction

The control theory known as Conditional Integrator (CI) was developed in a series of papers from Khalil and co-workers ([4], [2], [9], [8] and [6]). This controller acknowledges a saturation (natural or not) on the control signal, and takes advantage on that to behave, under some conditions, as an sliding mode controller (SMC). On other conditions, when not saturated, the controller behaves as a dynamical feedback with an important integral term. This approach has some interesting features, For example well known drawbacks of integrators like performance degradation and in particular the problem of integrator wind-up are avoided by the conditional nature of such control scheme. The integral action is then only present inside a boundary given by the saturations. In this way the control scheme assures the good properties of robustness and performance of sliding modes controllers for large errors, while allowing a smooth behavior given by its continuity what avoids chattering. Furthermore, the robustness of the SMC-like nature of the system while saturated is combined with the "adaptive" characteristic of the integral term when closer to equilibrium. In this way, such technique is very interesting in cases with poorly known systems or with uncertainties.

More recently ([12], [8] and [6]), efforts were consecrated to extend these results for the Multi-Input Multi-Output (MIMO) case, with good results for some classes of MIMO nonlinear systems. The present work follows this line and can be seen as an extension of those. This present work was motivated by airspace applications which in the first hand poorly known models and parameters, so CI is an interesting control strategy, while being an example of a class not addressed by previous results.

This paper will introduce in section II the considered class of MIMO nonlinear systems, and will present the main results that develop the CI controller for this class, mostly based on the nonlinear theory found in [3], [5] and [1]. These results are applied in III for the control of a MIMO nonlinear aircraft model. This result should be seen in the optics of the recent results ([10] and [12]) that have applied the conditional integrator controller to airspace, but in a SISO framework for the first and a MIMO framework for a linearized case of the second. Computer simulations are presented in section IV to illustrate the theoretical results. These simulations also compare the present results to those of [12] in order to illustrate the extension attained in the current work. The paper is then wrapped up by conclusions and perspectives in section V.

Gilney Damm is with IBISC - Université d'Evry Val d'Essonne, Evry, France gilney.damm@ibisc.fr

Van Cuong Nguyen is with IBISC - Université d'Evry Val d'Essonne, Evry, France vancuong.nguyen@ibisc.fr

II. Conditional integrator control design

The conditional integrator controller design for the output regulation of a class of minimum-phase nonlinear systems in case of asymptotically constant references is studied in [6], [8] and [9]. The works of these papers concern a servo-compensator performing as a sliding mode controller outside the boundary layer, and performing as a conditional one that provides servo-compensation only inside the boundary layer; achieving asymptotic output regulation. However, these works studied on the asymptotic stability of system inside the boundary layer without disturbance. The purpose of this section is then to present the conditional integrator controller design for the output regulation of MIMO nonlinear systems in case of asymptotically constant references without disturbances with the proof of the exponential stability of the system for some assumptions defined later.

Consider the nonlinear Multi-Input Multi-Output (MIMO) system in canonical form:

$$\left\{\begin{array}{lcl} \dot{x}_1 & = & x_2 \\ \dot{x}_2 & = & f(x_1,x_2)+g(x_1,x_2)u \\ y & = & x_1 \end{array}\right. \quad (1)$$

where $x_1 \in R^n$ and $x_2 \in R^n$ are the state vector, $y \in R^n$ the output vector, $u \in R^n$ the control input and $f(x_1,x_2) \in R^n$, $g(x_1,x_2) \in R^{n\times n}$ are continuous functions.

Let $y_{ref} = x_{1ref}$ be a prescribed reference output function considered as constant such that their derivatives are null. The asymptotic tracking problem consists in specifying a dynamic controller which depends on the desired output, its derivatives and the state variables and which steers the system output to asymptotically converge towards the reference.

Define the tracking error vector $e_1(t)$ as the difference between the actual system output $y(t) = x_1(t)$ and the reference output $e_1 = x_1 - x_{1ref}$, $e_2 = \dot{e}_1 = x_2 - \dot{x}_{1ref} =$

x_2, (1) can be rewritten as[1]:

$$\begin{cases} \dot{e}_1 &= e_2 \\ \dot{e}_2 &= f(e_1,e_2)+g(e_1,e_2)u \end{cases} \quad (2)$$

Let us impose the sliding surface with the intervention of the servo-compensation

$$s = k_0\sigma + K_1 e_1 + e_2 \quad (3)$$

where σ is the output of the conditional servo-compensator

$$\dot{\sigma} = -k_0\sigma + \mu sat(s/\mu) \quad (4)$$

in which μ is the boundary layer, k_0 is a positive parameter, $K_1 \in R^{n\times n}$ is chosen such a way that K_1+s is Hurwitz. The saturation function is determined as:

$$sat(s/\mu) = \begin{cases} s/\|s\| & \text{if } \|s\| \geq \mu \\ s/\mu & \text{if } \|s\| < \mu \end{cases} \quad (5)$$

The derivative of the sliding surface can be expressed as:

$$\dot{s} = k_0\dot{\sigma} + K_1\dot{e_1} + \dot{e_2} \quad (6)$$

Equation (6) may be written again from (2) and (3)

$$\begin{aligned} \dot{s}=&k_0(-k_0\sigma+\mu sat(s/\mu)) + K_1e_2 + \dot{e}_2 \\ =&k_0(-k_0(s-(K_1e_1+e_2))/k_0 + \mu sat(s/\mu)) + K_1e_2 + \dot{e}_2 \\ =&-k_0s + k_0\mu sat(s/\mu) + K_1e_2 + \dot{e}_2 + k_0(K_1e_1+e_2) \end{aligned} \quad (7)$$

Now by letting

$$\Delta(e_1,e_2) = k_0(K_1e_1+e_2) + K_1e_2 + f(e_1,e_2) \quad (8)$$

Equation (7) becomes

$$\dot{s} = -k_0s + k_0\mu sat(s/\mu) + \Delta(e_1,e_2) + g(e_1,e_2)u \quad (9)$$

The controller u is defined:

$$u = -\Pi(e_1,e_2)sat(s/\mu) \quad (10)$$

This controller allows to robustly stabilize the system (2) in a semi-global manner.

Proof: We will now demonstrate that control law defined in (10) can stabilize the class of nonlinear MIMO systems defined in (2). This proof is decomposed in two parts representing the region internal and external to the boundary layer.

Part 1: Inside the region $\|s\| \geq \mu$, $sat(s/\mu) = s/\|s\|$.

In this part, we demonstrate that the control law in (10) with $\Pi(\cdot)$ defined later in (14) will take the sliding surface inside the boundary layer. Before proceeding further, we introduce the following assumption.

Assumption 1: $\Delta(e_1,e_2)$ is bounded by a function of $\gamma(e_1,e_2)$ (where $\gamma(\cdot)$ is a function of class $\mathcal{K}$ function) and a positive constant Δ_0 :

$$\|\Delta(e_1,e_2)\| \leq \gamma(e_1,e_2) + \Delta_0 \quad (11)$$

for $(e_1,e_2) \in R^n \times R^n$ and while the sliding surface does not enter the boundary layer, i.e.$\|s\| \geq \mu$.

[1]For a simpler notation, we skip x_{ref}, $\dot{x}_{ref}$ and $\ddot{x}_{ref}$ inside $f(\cdot)$ and $g(\cdot)$.

Lets now consider the product $s^T\dot{s}$

$$\begin{aligned} s^T\dot{s} = &-s^Tk_0s + k_0\mu s^T sat(s/\mu) + s^T\Delta(e_1,e_2) \\ &+s^Tg(e_1,e_2)u \end{aligned} \quad (12)$$

This product $s^T\dot{s}$ can be developed with the previous assumption and the definition of saturation function (5):

$$\begin{aligned} s^T\dot{s}=&-s^Tk_0s + k_0\mu s^Ts/\|s\| + s^T\Delta(\cdot) - \Pi(\cdot)s^Tg(\cdot)s/\|s\| \\ \leq&-k_0s^Ts + k_0\mu s^Ts/\|s\| + \|\Delta(\cdot)\|\|s\| \\ &-\|g(\cdot)\|\Pi(\cdot)s^Ts/\|s\| \\ \leq&-k_0\|s\|^2 - (\lambda\Pi(\cdot) - \gamma(\cdot) - k_0\mu - \Delta_0)\|s\| \\ \leq&-k_0\|s\|^2 - \lambda\Pi_0\|s\| \end{aligned} \quad (13)$$

where we define

$$\Pi(\cdot) = \Pi_0 + (\gamma(\cdot) + k_0\mu + \Delta_0)/\lambda \quad (14)$$

the product $s^T\dot{s}$ is then not positive and

$$\begin{cases} s^T\dot{s} \leq -k_0\|s\|^2 - \lambda\Pi_0\|s\| \leq -\lambda\Pi_0\|s\| \\ \frac{d\|s\|}{dt} = \frac{\sqrt{s^Ts}}{dt} \leq -\lambda\Pi_0 \\ \|s(t)\| \leq \|s(0)\| - \lambda\Pi_0 t \end{cases} \quad (15)$$

Then the sliding surface $s(t)$ reaches the set $\|s(t)\| \leq \mu$ in finite time.

□

Part 2: In the region $\|s\| \leq \mu$, $sat(s/\mu) = s/\mu$.

In the following we denote $\mathcal{O}_\mu$ the region in the neighborhood of $(0,0)$ with a radius R_μ.

$$\mathcal{O}_\mu = \{e=(e_1,e_2) \in R^n \times R^n \mid \|e\| \leq R_\mu\} \quad (16)$$

Consider again (3), (15), (9) and control law (10). Inside the boundary layer, they may be rewritten as (17), it is useful to remind that $\dot{e}_1 = e_2$.

$$\begin{cases} \dot{\sigma} = -k_0\sigma + s \\ \dot{e}_1 = -K_1e_1 + s - k_0\sigma \\ \dot{s} = \Delta(\cdot) - g(\cdot)\Pi(\cdot)s/\mu \end{cases} \quad (17)$$

System (17) has an equilibrium point: $e_1 = 0$, $e_2 = 0$, $s = \bar{s}$ and $\sigma = \bar{\sigma}$ with $\bar{s} = k_0\bar{\sigma} = \mu\frac{g^{-1}(0,0)f(0,0)}{\Pi(0,0)}$ which implies in the design condition.

$$\|\bar{s}\| \leq \mu \Rightarrow \|(g^{-1}(0,0)f(0,0)\| \leq \Pi(0,0) \quad (18)$$

This condition is satisfied by control law (14).

System (17) may be rewritten with the intervention of $\bar{s}$ and $\bar{\sigma}$:

$$\begin{cases} \dot{\tilde{\sigma}} = -k_0\tilde{\sigma} + \tilde{s} \\ \dot{e}_1 = -K_1e_1 + \tilde{s} - k_0\tilde{\sigma} \\ \dot{\tilde{s}} = \Delta(\cdot) - \Pi(\cdot)g(\cdot)\tilde{s}/\mu - \Pi(\cdot)g(\cdot)\bar{s}/\mu \end{cases} \quad (19)$$

where $\tilde{\sigma} = \sigma - \bar{\sigma}$, $\tilde{s} = s - \bar{s}$.

In order to show that state variables of the system in (19) is tracked to the equilibrium point when applied by the control law in (10) with $\Pi(\cdot)$ defined later in (14) inside the boundary layer, some assumptions are presented as follow.

Assumption 2: function $g(e_1,e_2)$ satisfies two hypothesis:

Hypothesis 1: for $(e_1, e_2) \in R^n \times R^n$

$$g(e_1, e_2) + g^T(e_1, e_2) \geq 2\lambda I_n \text{ with the constant } \lambda > 0 \tag{20}$$

and the $n \times n$ identity matrix I_n.

Hypothesis 2: Inside the region $(e_1, e_2) \in \mathcal{O}_\mu$, function $g(e_1, e_2)$ satisfies the Lipschitz-like condition:

$$\|g(e_1, e_2) - g(0,0)\|\|f(0,0)\| \leq \|g(0,0)\|\upsilon(e_1, e_2) \tag{21}$$

A development of (21) gives us an alternative form for this hypothesis:

$$\|g(e_1, e_2)g^{-1}(0) - I_n\|\|f(0)\| \quad \leq \quad \upsilon(e_1, e_2) \tag{22}$$

in which, $\upsilon(e_1, e_2)$ is a suitable function satisfying

$$\upsilon(e_1, e_2) \quad = \quad \upsilon_1\|e_1\| + \upsilon_2\|e_2\| \leq K_\upsilon \tag{23}$$

where υ_1, υ_2 and K_υ are suitable positive constants.

□

Assumption 3: Inside the boundary layer, i.e.$\|s\| \leq \mu$, function $f(\cdot)$ is Lipschitz, such that:

$$\|f(e_1, e_2) - f(0,0)\| \leq l_1\|e_1\| + l_2\|e_2\| \tag{24}$$

where l_1 and $l_2 \in R^+$.

□

Assumption 4: Inside the boundary layer, i.e.$\|s\| \leq \mu$, function $\Pi(\cdot)$ satisfies:

$$\Pi(\cdot) - \Pi(0,0) \leq \chi(\cdot) = \lambda\chi_1\|e_1\| + \lambda\chi_2\|e_2\| \tag{25}$$

where χ_1, χ_2 are suitable positive constants and λ is defined early in (20).

□

We would like to demonstrate that every trajectory will be approached to the equilibrium point as time tends to infinity in the case inside the boundary layer. Toward that end, we take

$$W = \frac{\lambda_1}{2}\tilde{\sigma}^T\tilde{\sigma} + \frac{\lambda_2}{2}e_1^Te_1 + \frac{\tilde{s}^T\tilde{s}}{2} \tag{26}$$

as a Lyapunov candidate, where λ_1 and λ_2 are positive constants.

Its derivative can be easily calculated as:

$$\begin{aligned}\dot{W}=&\lambda_1\tilde{\sigma}^T\dot{\tilde{\sigma}} + \lambda_2 e_1^T\dot{e_1} + \tilde{s}^T\dot{\tilde{s}}\\ =&\lambda_1\tilde{\sigma}^T(-k_0\tilde{\sigma} + \tilde{s}) + \lambda_2 e_1^T(-K_1e_1 + \tilde{s} - k_0\tilde{\sigma})\\ &+\tilde{s}^T(\Delta(\cdot) - \Pi(\cdot)g(\cdot)\tilde{s}/\mu - \Pi(\cdot)g(\cdot)\bar{s}/\mu)\end{aligned} \tag{27}$$

Since $(e_1, e_2) \in \mathcal{O}_\mu$, $\Delta(\cdot)$ can be expressed:

$$\begin{aligned}\Delta(\cdot) \quad &= \quad k_0(s - k_0\sigma) + K_1(-K_1e_1 + s - k_0\sigma) + f(\cdot)\\ &= \quad k_0\tilde{s} - k_0^2\tilde{\sigma} - K_1^2e_1 + K_1\tilde{s} - k_0K_1\tilde{\sigma} + f(\cdot)\end{aligned} \tag{28}$$

then,

$$\begin{aligned}\dot{W}=&\lambda_1\tilde{\sigma}^T(-k_0\tilde{\sigma} + \tilde{s}) + \lambda_2 e_1^T(-K_1e_1 + \tilde{s} - k_0\tilde{\sigma})\\ &+\tilde{s}^T(k_0\tilde{s} - k_0^2\tilde{\sigma} - K_1^2e_1 + K_1\tilde{s} - k_0K_1\tilde{\sigma}\\ &-\Pi(\cdot)g(\cdot)\tilde{s}/\mu) + \tilde{s}^T(f(\cdot) - \Pi(\cdot)g(\cdot)\bar{s}/\mu)\end{aligned} \tag{29}$$

In order to express the derivative of Lyapunov candidate more clearly, we consider firstly the term:

$$\begin{aligned}&\|f(\cdot) - \Pi(\cdot)g(\cdot)\bar{s}/\mu\| = \|f(\cdot) - \tfrac{\Pi(\cdot)}{\Pi(0,0)}g(\cdot)g^{-1}(0,0)f(0,0)\|\\ &= \|f(\cdot) - f(0,0) - \tfrac{\Pi(\cdot)}{\Pi(0,0)}[g(\cdot)g^{-1}(0,0) - I_n]f(0,0)\\ &-\tfrac{\Pi(\cdot)-\Pi(0,0)}{\Pi(0,0)}f(0,0)\|\\ &\leq \|f(\cdot) - f(0,0)\| + \tfrac{\Pi(\cdot)}{\Pi(0,0)}\|g(\cdot)g^{-1}(0,0) - I_n\|\|f(0,0)\|\\ &+\tfrac{\Pi(\cdot)-\Pi(0,0)}{\Pi(0,0)}\|f(0,0)\|\end{aligned} \tag{30}$$

using assumptions 2, 3, 4 and the relation in (23), the previous expression can be expressed as:

$$\begin{aligned}&\|f(\cdot) - \Pi(\cdot)g(\cdot)\bar{s}/\mu\|\\ &\leq l_1\|e_1\| + l_2\|e_2\| + \tfrac{\Pi(\cdot)}{\Pi(0,0)}\upsilon(\cdot) + \tfrac{\chi(\cdot)\|f(0,0)\|}{\lambda\Pi(0,0)}\\ &\leq l_1\|e_1\| + l_2\|e_2\| + \upsilon(\cdot) + \tfrac{\chi(\cdot)\upsilon(\cdot)}{\lambda\Pi(0,0)} + \tfrac{\chi(\cdot)\|f(0,0)\|}{\lambda\Pi(0,0)}\\ &\leq l_1\|e_1\| + l_2\|e_2\| + \upsilon(\cdot) + \tfrac{(\|f(0,0)\|+K_\upsilon)\chi(\cdot)}{\lambda\Pi(0,0)}\\ &\leq (l_1 + \upsilon_1 + (\|f(0,0)\| + K_\upsilon)\tfrac{\chi_1}{\Pi(0,0)})\|e_1\| + (l_2 + \upsilon_2\\ &+(\|f(0,0)\| + K_\upsilon)\tfrac{\chi_2}{\Pi(0,0)})\|e_2\|\end{aligned} \tag{31}$$

Let us define $c_1 = l_1 + \upsilon_1 + (\|f(0,0)\| + K_\upsilon)\frac{\chi_1}{\Pi(0,0)}$ and $c_2 = l_2 + \upsilon_2 + (\|f(0,0)\| + K_\upsilon)\frac{\chi_2}{\Pi(0,0)}$, this expression may be rewritten as:

$$\begin{aligned}&\|f(\cdot) - \Pi(\cdot)g(\cdot)\bar{s}/\mu\|\\ &\leq c_1\|e_1\| + c_2\|e_2\|\\ &\leq (c_1 + c_2\|K_1\|)\|e_1\| + c_2\|\tilde{s}\| + k_0c_2\|\tilde{\sigma}\|\end{aligned} \tag{32}$$

From (19) and (32) the derivative of W can be developed:

$$\begin{aligned}\dot{W}=&-\lambda_1k_0\tilde{\sigma}^T\tilde{\sigma} + \lambda_1\tilde{\sigma}^T\tilde{s} - \lambda_2e_1^TK_1e_1 + \lambda_2e_1^T\tilde{s} - \lambda_2k_0e_1^T\tilde{\sigma}\\ &+k_0\tilde{s}^T\tilde{s} - k_0^2\tilde{s}^T\tilde{\sigma} - \tilde{s}^TK_1^2e_1 + \tilde{s}^TK_1\tilde{s} - k_0s^TK_1\tilde{\sigma}\\ &-\Pi(\cdot)\bar{s}^Tg(\cdot)\tilde{s}/\mu + \tilde{s}^T(f(\cdot) - \Pi(\cdot)g(\cdot)\bar{s}/\mu)\\ \leq&-\tfrac{\lambda_1}{2}(\|\tilde{s}\| - \|\tilde{\sigma}\|)^2 - \tfrac{\lambda_2}{2}(\|\tilde{s}\| - \|e_1\|)^2 - \tfrac{\lambda_2k_0}{2}(\|\tilde{\sigma}\| - \|e_1\|)^2\\ &-\tfrac{k_0^2}{2}(\|\tilde{\sigma}\| - \|\tilde{s}\|)^2 - \tfrac{\|K_1^2\|}{2}(\|e_1\| - \|\tilde{s}\|)^2\\ &-\tfrac{k_0\|K_1\|}{2}(\|\tilde{\sigma}\| - \|\tilde{s}\|)^2 - \tfrac{c_1+c_2\|K_1\|}{2}(\|e_1\| - \|\tilde{s}\|)^2\\ &-\tfrac{c_2\|K_1\|}{2}(\|e_1\| - \|\tilde{s}\|)^2 - \tfrac{k_0c_2}{2}(\|\tilde{\sigma}\| - \|\tilde{s}\|)^2\\ &-(\lambda_1k_0 - \tfrac{1}{2}(\lambda_1 + \lambda_2k_0 + k_0^2 + k_0\|K_1\| + k_0c_2))\|\tilde{\sigma}\|^2\\ &-(\lambda_2\|K_1\| - \tfrac{1}{2}(\lambda_2 + \lambda_2k_0 + \|K_1^2\| + c_1 + c_2\|K_1\|))\|e_1\|^2\\ &-(\Pi(\cdot)\|g(\cdot)\|/\mu - \tfrac{1}{2}(\lambda_1 + \lambda_2 + k_0 + k_0^2 + \|K_1^2\| + \|K_1\|\\ &+k_0\|K_1\| + c_1 + c_2\|K_1\| + c_2 + k_0c_2))\|\tilde{s}\|^2\end{aligned} \tag{33}$$

It can be verified that by taking λ_1, λ_2 and $\Pi(\cdot)$ large enough and μ small enough, the following conditions are satisfied:

$$\begin{cases}\lambda_1k_0 - 1/2(\lambda_1 + \lambda_2k_0) > 1/2(k_0^2 + k_0\|K_1\| + k_0c_2)\\ \lambda_2\|K_1\| - 1/2(\lambda_2 + \lambda_2k_0) > 1/2(\|K_1^2\| + c_1 + c_2\|K_1\|)\\ \Pi(\cdot)\|g(\cdot)\|/\mu - 1/2(\lambda_1 + \lambda_2) > 1/2(k_0 + k_0^2 + \|K_1^2\| + \|K_1\|\\ +k_0\|K_1\| + c_1 + c_2\|K_1\| + c_2 + k_0c_2)\end{cases} \tag{34}$$

In this way, $W(t)$ satisfies $W(t) > 0$ and $\dot{W} < -w_0W$ (where w_0 is a positive constant) for all $\sigma \neq \bar{\sigma}$, $e_1 \neq 0$ and $s \neq \bar{s}$. Then $W(t)$ reaches exponentially zero when time tends to infinite. As consequence, the output error $e_1(t)$ tends to zero and σ and s tend to their equilibrium values as time tends to infinite. We may assure the exponential stability of the system in the region of $\|s\| \leq \mu$.

The stability of system (1) is verified for the conditional integrator control designed in (10).

■

We can then state the results developed above in the form of the theorem:

Theorem *2.1:* A class of Multi-Input Multi-Output nonlinear systems described by (1), and satisfying assumptions (1-4) can be stabilized semi-globally to their constant reference by the controller (10-3-4-14) with tunning parameters (Π_0, k_0, μ and K_1 defined in the previous section) and function $\gamma(\cdot)$ conveniently set. Furthermore, the stability is exponential inside an error region defined in (16).

■

In the following section we will apply this result to a nonlinear MIMO aircraft control problem. The linearized version of this problem is already addressed in [12].

III. Example: F-16 aircraft's lateral mode control design

In this section, we address the control of a nonlinear MIMO system applying the results obtained in the previous section. The considered system is the nonlinear MIMO model of an F-16 aircraft lateral mode. The work of [12] has addressed this case designing a conditional integrator based on the linearization of the system around an operating point. In the present case, we extend those results and those of [6] addressing the nonlinear MIMO system without linearization.

The F-16 aircraft lateral mode has two inputs (aileron and rudder) and two outputs (sideslip angle and roll angle). In this way, only lateral state variables are time varying. Others longitudinal state variables (like height and pitch) are considered as constant or null. The lateral dynamic model used to the control design procedure is consequently reduced as below (see [14] and [11]):

$$\begin{cases} \dot{\beta}=\frac{1}{mV}(-\cos(\alpha_0)\sin(\beta)(T+C_x(\alpha_0)\bar{q}S) \\ \quad +\cos(\beta)C_y(\beta)\bar{q}S-\sin(\alpha_0)\sin(\beta)C_z(\alpha_0,\beta)\bar{q}S) \\ \quad +\sin(\alpha_0)p-\cos(\alpha_0)r+\frac{\rho S}{4m}(\cos(\beta)C_{y_p}(\alpha_0)\bar{b}p \\ \quad +\cos(\beta)C_{y_r}(\alpha_0)\bar{b}r)+\frac{g}{V}(\cos(\alpha_0)\sin(\beta)\sin(\theta_0) \\ \quad +\cos(\beta)\cos(\theta_0)\sin(\phi)-\sin(\alpha_0)\sin(\beta)\cos(\phi)) \\ \dot{\phi}=p+\cos(\phi)\tan(\theta_0)r \\ \dot{p}=I_3C_l(\alpha_0,\beta)\bar{q}S\bar{b}+I_4C_n(\alpha_0,\beta)\bar{q}S\bar{b}+\frac{\rho VS\bar{b}}{4}[(I_3C_{l_p}(\alpha_0) \\ \quad +I_4C_{n_p}(\alpha_0))p+(I_3C_{l_r}(\alpha_0)+I_4C_{n_r}(\alpha_0))r] \\ \quad +\bar{q}S[(I_3C_{l_{\delta_a}}(\alpha_0)+I_4C_{n_{\delta_a}}(\alpha_0))\delta_a+(I_3C_{l_{\delta_r}}(\alpha_0) \\ \quad +I_4C_{n_{\delta_r}}(\alpha_0))\delta_r] \\ \dot{r}=I_4C_l(\alpha_0,\beta)\bar{q}S\bar{b}+I_9C_n(\alpha_0,\beta)\bar{q}S\bar{b}+\frac{\rho VS\bar{b}}{4}[(I_4C_{l_p}(\alpha_0) \\ \quad +I_9C_{n_p}(\alpha_0))p+(I_4C_{l_r}(\alpha_0)+I_9C_{n_r}(\alpha_0))r] \\ \quad +\bar{q}S[(I_4C_{l_{\delta_a}}(\alpha_0)+I_9C_{n_{\delta_a}}(\alpha_0))\delta_a+(I_4C_{l_{\delta_r}}(\alpha_0) \\ \quad +I_9C_{n_{\delta_r}}(\alpha_0))\delta_r] \end{cases} \tag{35}$$

In which, $\bar{b}$ is the equivalent length, S the equivalent wing surface, $I_{xx}, I_{yy}, I_{zz}, I_{xz}$ are the moments of inertia in kgm^2. $I_3 = \frac{I_{zz}}{(I_{xx}I_{zz}-I_{xz}^2)}$, $I_4 = \frac{I_{xz}}{(I_{xx}I_{zz}-I_{xz}^2)}$, $I_9 = \frac{I_{xx}}{(I_{xx}I_{zz}-I_{xz}^2)}$. m is the mass of the system (kg) and g the gravity constant, α_0, θ_0 and V are angle of attack, pitch angle and airspeed considered as constant in the studied case, T is the thrust force. The state variables of the system are β, ϕ, p, r which represent the sideslip angle, roll angle, roll rate, yaw rate, respectively. $C_y(\alpha_0)$, $C_{y_p}(\alpha_0)$, $C_{y_r}(\alpha_0)$, $C_l(\alpha_0,\beta)$, $C_n(\alpha_0,\beta)$, $C_{l_p}(\alpha_0)$, $C_{n_p}(\alpha_0)$, $C_{l_r}(\alpha_0)$, $C_{n_r}(\alpha_0)$, $C_{l_{\delta_a}}(\alpha_0)$, $C_{n_{\delta_a}}(\alpha_0)$, $C_{l_{\delta_r}}(\alpha_0)$, $C_{n_{\delta_r}}(\alpha_0)$ are lateral aerodynamic coefficients taken from [7]. Finally, the control inputs are respectively the aileron (δ_a) and the rudder (δ_r).

The equations system (35) can be rearranged as:

$$\begin{cases} \begin{bmatrix}\dot{\beta}\\ \dot{\phi}\end{bmatrix}=f_{11}(\beta,\phi)+f_{12}(\beta,\phi)\begin{bmatrix}p\\ r\end{bmatrix} \\ \begin{bmatrix}\dot{p}\\ \dot{r}\end{bmatrix}=f_{21}(\beta,\phi)+f_{22}(\beta,\phi)\begin{bmatrix}p\\ r\end{bmatrix}+g_2(\beta,\phi)\begin{bmatrix}\delta_a\\ \delta_r\end{bmatrix} \end{cases} \tag{36}$$

where $f_{11}(\cdot)$, $f_{12}(\cdot)$, $f_{13}(\cdot)$, $f_{21}(\cdot)$, $f_{22}(\cdot)$, and $g_2(\cdot)$ represent the terms of (35) respectively. Equation (36) is mainly used for controller design and stability analysis.

Let us define $x_1 = [\beta, \phi]^T$, $x_2 = \dot{x}_1 = [\dot{\beta}, \dot{\phi}]^T$ and $u = [\delta_a, \delta_r]^T$. (36) can be written again as:

$$\begin{cases} \dot{x}_1 = x_2 \\ \dot{x}_2 = F^{'}(x_1,x_2)+G^{'}(x_1,x_2)u \end{cases} \tag{37}$$

where

$$\begin{cases} F^{'}(\cdot) = (\frac{\partial f_{11}(\cdot)}{\partial x_1}+(f(\cdot)+f_{12}(\cdot)f_{22}(\cdot))(f_{12}(\cdot))^{-1})x_2 \\ \qquad -(f(\cdot)+f_{12}(\cdot)f_{22}(\cdot))(f_{12}(\cdot))^{-1}f_{11}(\cdot) \\ \qquad +f_{12}(\cdot)f_{21}(\cdot) \\ G^{'}(\cdot) = f_{12}(\cdot)g_2(\cdot) \\ f(\cdot)\begin{bmatrix}p\\ r\end{bmatrix}=\frac{\partial(f_{12}(\cdot)\begin{bmatrix}p\\ r\end{bmatrix})}{\partial x_1} \end{cases} \tag{38}$$

Let $y_{ref} = x_{1ref} = [\beta_{ref}, \phi_{ref}]^T$ be a prescribed reference output considered as constant function and $y(t) = x_1(t)$ is the actual output. In order to design the MIMO conditional integrator controller, we define output error vector $e_1 = x_1 - x_{1ref}$ and $e_2 = \dot{e}_1$. (38) can be transformed into (39) with the intervention of two new state variables e_1 and e_2.

$$\begin{cases} \dot{e}_1 = e_2 \\ \dot{e}_2 = F(e_1,e_2)+G(e_1,e_2)u \end{cases} \tag{39}$$

$G(x_1,x_2)$ is invertible for $\beta \in (-20°, 20°)$, $\phi \in (-60°, 60°)$ and $\alpha \in (-10°, 45°)$, and we also suppose that $F(x_1,x_2)$ is smooth. Application of control law in (10) for the system in (39) gives us the controller:

$$\begin{cases} u = -\Pi(e_1,e_2)sat(s/\mu) \\ \Pi(\cdot) = \Pi_0+(\gamma(\cdot)+k_0\mu+\Delta_0)/\lambda \end{cases} \tag{40}$$

with

$$\begin{cases} s = k_0\sigma+K_1e_1+e_2 \\ \dot{\sigma} = -k_0\sigma+\mu sat(s/\mu) \end{cases} \tag{41}$$

where $\lambda = min(\|G(\cdot)\|)$ for $\beta \in (-20°, 20°)$ and $\phi \in (-60°, 60°)$. Δ_0 is a positive constant, Π_0 is a positive parameter large enough, k_0 is a positive parameter, μ is the boundary layer small enough and K_1 is chosen such a way that $K_1 + s$ is Hurwitz. All Π_0, k_0, μ, K_1 and $\gamma(\cdot)$ are to be determined.

IV. Simulation Results

In sections II and III, the design methodology of the conditional integrator controller to track sideslip angle and roll angle is proposed taking into account the full aerodynamic characteristics of the lateral mode of an F-16 aircraft. This section presents numerical simulation results for the controller to illustrate the performance of the proposed conditional integrator control laws.

As mentioned in section III, we use the lateral mode F-16 nonlinear model in this paper. This because its nonlinear model, wind tunnel informations and data are widely known and used for control design. It is important to remark that the model used in the following simulations is even more complete than that used in the control design, for example it includes actuator dynamics and their limitations. As a consequence, simulations also illustrate some properties of robustness to unmodeled dynamics.

In the following simulations, we have applied the MIMO conditional integrator controller for controlling the sideslip and roll angle of the lateral mode of the F-16 aircraft model. We may note that the control inputs are always limited by $|\delta_a| < 21^\circ$ and $|\delta_r| < 30^\circ$, which represent the physical limitations of these actuators.

The system is studied at the operating point $(V, h) = (153m/s, 7162m)$ corresponding to the trimmed angle of attack $\alpha_0 = 2.1^\circ$, pitch angle $\theta_0 = 2.1^\circ$, sideslip $\beta_0 = 0^\circ$, $\phi_0 = 0^\circ$ and to trimmed control surface values: aileron $\delta_a = 0^\circ$ and rudder $\delta_r = 0^\circ$.

The control law in (40) whose $\Pi(\cdot)$ can be written in a more simple form as below:

$$\Pi(\cdot) = \Pi_0 + \gamma(\cdot) \tag{42}$$

in which, $\gamma(\cdot) = \gamma_1\|e_1\| + \gamma_2\|e_2\|$, γ_1 and γ_2 are positive constant.

Application of this control law to lateral mode presented in section (III) is done by determining the set of parameters Π_0, γ_1, γ_2, μ, K_1 and k_0 in Table I. It is interesting to note that Π_0 and k_0 are defined in matrix form because of the difference in dynamic property of two state variables <sideslip> and <roll angle>. This definition does not have any consequence on the stability of the system.

Π_0	μ	γ_1 and γ_2	k_0	K_1
$\begin{bmatrix} 20 & 0.0 \\ 0.0 & 20 \end{bmatrix}$	1.0	0.0 and 0.0	$\begin{bmatrix} 2.6 & 0.0 \\ 0.0 & 3.5 \end{bmatrix}$	$\begin{bmatrix} 2.0 & 0.0 \\ 0.0 & 3.2 \end{bmatrix}$

TABLE I

Parameters for the lateral mode

The reference input is taken as in [12] and [13] with a small change in its amplitude. It consists of two step changes in sideslip and roll angles at $t = 8s$ and at $t = 30s$ as:

$$\begin{bmatrix} \beta_{ref}(t) \\ \phi_{ref}(t) \end{bmatrix} = \begin{bmatrix} 0.3(-\frac{0.5}{1+e^{t-8}} + \frac{1}{1+e^{t-30}} - 0.5) \\ 0.3(-\frac{0.5}{1+e^{t-8}} + \frac{1}{1+e^{t-30}} - 0.2) \end{bmatrix} \tag{43}$$

Two initial conditions of sideslip and roll angle are studied. The first corresponds to a small initial condition of sideslip and roll angle ($\beta_0 = 0^\circ, \phi_0 = 5^\circ$) to the equilibrium point, and the second corresponds to a high one ($\beta_0 = 10^\circ, \phi_0 = 20^\circ$) from the equilibrium point.

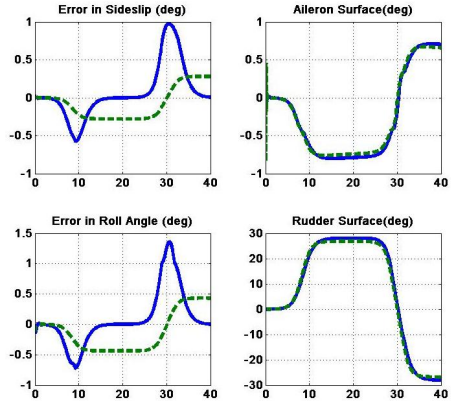

Fig. 1. Output Errors and Control Surfaces for a small initial condition. CI (solid) - SMC (dashed)

The plots in Fig. 1 and Fig. 2 are obtained with the controller structure described in section III (solid lines) which is compared to a sliding mode controller (dashed lines) where the sign function is replaced by a saturation function to avoid chattering. This controller is used to regulate sideslip angle and roll angle errors. Fig. 1 represents the system output errors in respect to references. The conditional integrator controller provides a convergence to zero of the output error (solid lines) for both sideslip and roll angle in the two cases of initial conditions. In contrast, the sliding mode controller (SMC) produces an output error (dash lines) with non-zero steady state error. This well illustrate the positive contribution of integral term to recover steady state information.

The benefit of the proposed controller is even more clear in the case of high initial conditions where the SMC bring the system to a not constant behaviour, even if still stable.

Fig. 2 shows the control surfaces of the system for both

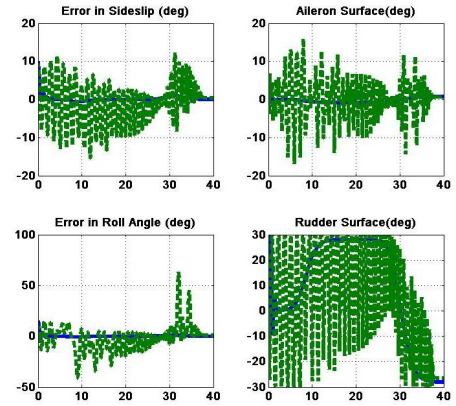

Fig. 2. Output Errors and Control Surfaces for a high initial condition. CI (solid) - SMC (dashed)

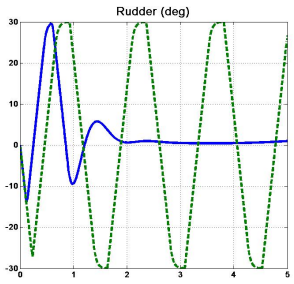

Fig. 3. Detail on Control Surface (Rudder) for a high initial condition. CI (solid) - SMC (dashed)

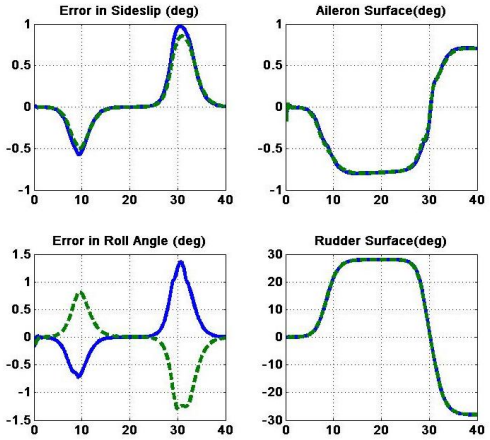

Fig. 4. Output Errors and Control Surfaces for a small initial condition. CI (solid) - Controller in [12] (dashed)

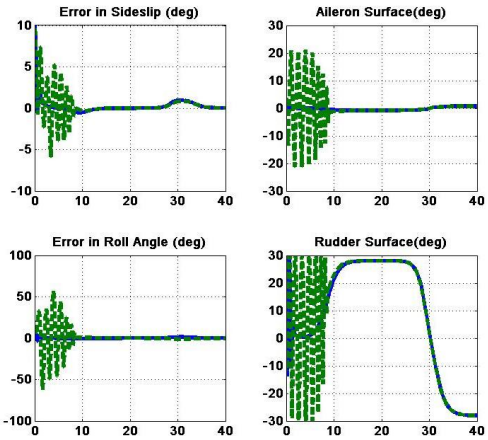

Fig. 5. Output Errors and Control Surfaces for a high initial condition. CI (solid) - Controller in [12] (dashed)

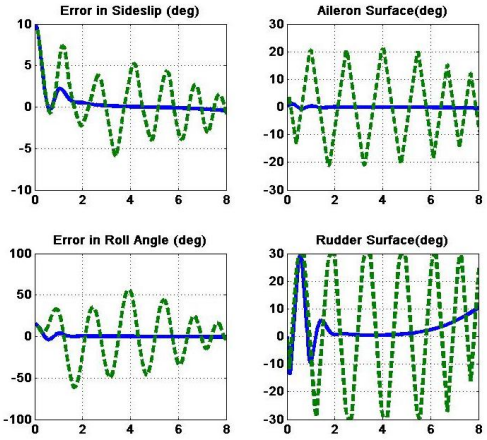

Fig. 6. Detail on Output Errors and Control Surfaces for a high initial condition. CI (solid) - Controller in [12] (dashed)

controllers. The solid lines correspond to control surfaces (aileron and rudder) of conditional integrator controller. The dash lines represent control surfaces of conditional integrator controller.

We present a detail of Fig. 2 in Fig. 3. There is quite clear the mechanism of the conditional integrator. One may observe that for large initial conditions, the system is driven to the boundary layer where it is captured by the exponential convergent property of the controller. From there on, the controller behaves in a very smooth way.

The plots in Fig. 4 to Fig. 5 are obtained with the controller structure described in section III and the controller designed in [12] for the F-16 aircraft lateral mode, linearized at the same equilibrium point ($V = 153m/s, \alpha = 2.1°$) used to regulate sideslip angle and roll angle errors. All parameters are obtained from [12].

The two controllers give the same output error and control surfaces (aileron and rudder) for the case of small initial conditions (Fig. 4). That demonstrate the good performance of both controllers. For high initial conditions, the controller in [12] based on linearizations may have very large oscillations (up to $50°$ in Fig. 5). Moreover, Figs 6 that presents a closer view of Fig. 5 well illustrate the behavior of the controller, with an exponential convergence since entering a residual region, obtaining better a transitory for large initial conditions.

V. Conclusion

This paper has developed a conditional integrator controller for a class of MIMO nonlinear systems. Conditional integrators are an interesting solution for particular uncertain problems largely found in practice, and specially in airspace. This control technique has been developed in a series of papers found in literature in the last decade.

The present work intends to extend then for a class of MIMO nonlinear systems strongly motivated by airspace problems. The main results are summarized in a theorem concerning a general class of systems, and shows that for mild and easily fulfilled assumptions, these systems can be semi-globally stabilized in finite time towards a region of the state space. Finally, the controller exponentially stabilizes the system inside this region to its equilibrium. The resulting controller was applied to an example of aircraft control, and its performance as well as the contributions compared

to previous works found in the literature are illustrated by computer simulations. These results are currently being applied to more general and complex airspace problems with very interesting results. Flight tests are expected to be carried out in a near future to corroborate theoretical results.

REFERENCES

[1] Alberto Isidori. *Nonlinear Control Systems*. Springer Verlag, 1995.

[2] Hassan K. Khalil. On the design of robust servomechanisms for minimum phase nonlinear systems. *Robust Nonlinear Control 2000, John Wiley & Sons*, 10:339–361, 2000.

[3] Hassan K. Khalil. *Nonlinear Systems*. Prentice Hall, 2001.

[4] Nazmi A. Mahmoud and Hassan K. Khalil. Robust control for a nonlinear servomechanism problem. *IEEE - Transactions on Automatic Control*, 1996.

[5] Riccardo Marino and Patrizio Tomei. *Nonlinear Control Design: Geometric, Adaptive and Robust*. Prentice Hall, 1st edition, 1995.

[6] Attaullah Y. Memona and Hassan K. Khalil. Output regulation of nonlinear systems using conditional servocompensators. *Automatica*, 2010.

[7] Eugene Morelli. Global nonlinear parametric modeling with application to f-16 aerodynamics. *American Institute of Aeronautics and Astronautics*, 1998.

[8] Sridhar Seshagiri and Hassan K. Khalil. Robust output feedback regulation of minimum-phase nonlinear systems usingconditional integrators. *Automatica*, 2005.

[9] Sridhar Seshagiri and Hassan K. Khalil. Robust output regulation of minimum phase nonlinear systems using conditional servocompensators. *Wiley InterScience*, 2005.

[10] Sridhar Seshagiri and Ekprasit Promtun. Sliding mode control of f-16 longitudinal dynamics. *American Control Conference*, pages 1770–1775, 2008.

[11] Lars Sonneveldt. *Nonlinear F-16 Model Description*. Delft University of Technology, Netherlands, 2006.

[12] Hoa Vo and Sridhar Seshagiri. Robust control of f-16 lateral dynamics. *Industrial Electronics, 2008. IECON 2008. 34th Annual Conference of IEEE*, pages 343–348, 2008.

[13] Amanda Young, Chengyu Cao, and Naira Hovakimyan. An adaptive approach to nonaffine control design for aircraft applications. *AIAA Guidance, Navigation, and Control Conference and Exhibit*, 2006.

[14] Peter H. Zipfel. *Modeling and Simulation of Aerospace Vehicle Dynamics, 2nd edition*. American Institute of Aeronautics and Astronautics, 2000.